Weierstraß–Institut
für Angewandte Analysis und Stochastik

im Forschungsverbund Berlin e.V.

Preprint ISSN 0946 – 8633

On boundary conditions for multidimensional sedimentation-consolidation processes in closed vessels

Raimund Bürger[1], Matthias Kunik[2]

submitted: 23rd December 1999

[1] Institute of Mathematics A
University of Stuttgart
Pfaffenwaldring 57
D – 70569 Stuttgart
Germany
E-mail: buerger@mathematik.uni-stuttgart.de

[2] Weierstrass Institute
for Applied Analysis
and Stochastics
Mohrenstraße 39
D – 10117 Berlin
Germany
E-Mail: kunik@wias-berlin.de

Preprint No. 544
Berlin 1999

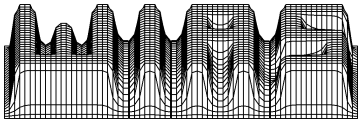

1991 Mathematics Subject Classification. 35K65, 35Q30, 76A99, 76T05.

Key words and phrases. Sedimentation-consolidation process; flocculated suspension; boundary conditions, inclied walls, Boykott effect.

Edited by
Weierstraß–Institut für Angewandte Analysis und Stochastik (WIAS)
Mohrenstraße 39
D — 10117 Berlin
Germany

Fax: + 49 30 2044975
E-Mail (X.400): c=de;a=d400-gw;p=WIAS-BERLIN;s=preprint
E-Mail (Internet): preprint@wias-berlin.de
World Wide Web: http://www.wias-berlin.de/

Abstract

The two-phase flow of a flocculated suspension in a closed settling vessel with inclined walls is investigated within the phenomenological theory of sedimentation-consolidation processes. We formulate possible wall boundary conditions and use these conditions to derive spatially one-dimensional field equations for planar flows and flows which are symmetric with respect to the vertical axis. For both kinds of flows we assume a general geometry of the sedimentation vessel and include the study of a compressible sediment layer. We analyze the special cases of a conical vessel, a roof-shaped vessel and a vessel with parallel inclined walls. The case of a small initial time and a large time for the final consolidation state leads to explicit expressions for the flow fields. From a mathematical point of view, the resulting initial-boundary value problems are well posed and can be solved numerically by a simple adaptation of one of the newly developed numerical schemes for strongly degenerate convection-diffusion problems. However, from a physical point of view, both the analytical and numerical results rise doubts concerning the validity of the general field equations. In particular, the strongly reduced form of the linear momentum balance seems to be an oversimplification. Included in our discussion as a special case are the Kynch theory and well-known analyses of sedimentation in vessels with inclined walls within the framework of kinematic waves, which exhibit similar shortcomings.

1 Introduction

Mathematical models describing the settling of flocculated suspensions are of great interest in numerous areas such as mineral processing, wastewater treatment and medicine. Although settling tanks that can be treated as a simple one-dimensional cylinder are rather the exception than the rule in these applications, most experimental and theoretical treatments of sedimentation problems have been limited to this simple case so far. Starting from the local mass and linear momentum balances for both the solid and liquid component, introducing appropriate constitutive assumptions and performing a dimensional analysis, BÜRGER et al. [13] derived a set of field equations for these processes in several space dimensions. However, they did not yet specify suitable boundary conditions for these equations. The present study is concerned with some problems related to the formulation of such boundary conditions.

To put the present work in the proper perspective, we recall that settling rates of suspensions of small particles in vessels with downward-facing walls can be several

times larger than in vessels with vertical walls. This well-known effect was first observed by BOYCOTT [5] in 1920 and is exploited frequently in industrial applications to enhance performance of solid-liquid separation equipment (see, e.g. [33, 34, 44]) and has been subject of a large number of experimental and theoretical studies. This effect is related to the formation of a thin upwards-streaming liquid boundary layer beneath downward-facing walls during sedimentation.

Overviews of early research work concerning the Boycott effect are given by ACRIVOS and HERBOLZHEIMER [1] and DAVIS and ACRIVOS [17]. A well-known elementary kinematic model describing this effect, the so-called PNK theory, was advanced independently by PONDER [41] and NAKAMURA and KURODA [37]. This theory states that the rate of production of clarified fluid is equal to the vertical settling velocity of the particles multiplied by the horizontal projection of the channel area available for settling (see [17]). In the sequel, numerous experiments with different materials were performed to verify this theory [21, 22, 27, 29, 39, 40, 50]. Some of these authors proposed corrections since the observed sedimentation enhancement was in general less than predicted by the PNK theory.

The first analysis of the phenomenon starting from the basic balance equations of continuum mechanics was presented by HILL et al. [24]. They studied the settling of dilute dispersions in conical vessels and also obtained numerical solutions showing details of the flow field. ACRIVOS and HERBOLZHEIMER [1] considered arbitrary concentrations and geometry of the settling vessel. They also found that the observed deviations of the settling velocities from those predicted by the PNK theory could be explained by a flow instability causing the particles to resuspend. We mention that ACRIVOS and HERBOLZHEIMER assume that the suspensions behaves as a Newtonian fluid with an effective viscosity depending on the local solids concentration. This is in contrast to the kinematic wave treatment by SCHNEIDER [46] which considers the inviscid case. On the other hand, while ACRIVOS and HERBOLZHEIMER [1] assume that the concentration in the bulk suspension is constant, SCHNEIDER's [46] analysis allows the formation of vertical concentration gradients. We point out that SHAQFEH and ACRIVOS [47, 48, 49] solve very general field equations for settling in vessels having inclined walls that are valid over a wide range of parameters, and that include both models presented in [1] and [46] as limiting cases. Sedimentation in inclined vessels gives rise to two types of boundary layers, namely the flow of clear fluid beneath upward-facing walls and the forming of a sediment layer on downward-facing walls. Analyses of flow phenomena related to these boundary layers include [4, 42] and [2, 28, 38], respectively. Finally, we mention analyses of sedimentation in narrow tilted channels [23] and in very narrow inclined fracture channels [35].

To outline the scope of the present paper in detail, it is necessary that we briefly recall some basic balance equations for the three-dimensional flow of a solid-liquid suspension. Following the approach of the theory of mixtures, both components are considered as superimposed continuous media [3]. The local mass balances for both

components read then

$$\frac{\partial \phi}{\partial t} + \nabla \cdot (\phi \mathbf{v}_\mathrm{s}) = 0, \quad \frac{\partial \phi}{\partial t} - \nabla \cdot \big((1-\phi)\mathbf{v}_\mathrm{f}\big) = 0, \tag{1}$$

where ϕ denotes the volumetric solids concentration and $\mathbf{v}_\mathrm{s}$ and $\mathbf{v}_\mathrm{f}$ are the respective solid and fluid phase velocities. Introducing the volume-average velocity

$$\mathbf{q} = \phi \mathbf{v}_\mathrm{s} + (1-\phi)\mathbf{v}_\mathrm{f}, \tag{2}$$

defining the solid-fluid relative velocity or drift velocity $\mathbf{v}_\mathrm{r} = \mathbf{v}_\mathrm{s} - \mathbf{v}_\mathrm{f}$ and noting that $\phi \mathbf{v}_\mathrm{s} = \phi \mathbf{q} + \phi(1-\phi)\mathbf{v}_\mathrm{r}$, we may rewrite equations (1) as

$$\frac{\partial \phi}{\partial t} + \nabla \cdot \big(\phi \mathbf{q} + \phi(1-\phi)\mathbf{v}_\mathrm{r}\big) = 0, \tag{3}$$

$$\nabla \cdot \mathbf{q} = 0. \tag{4}$$

The properties of the material considered are represented by a constitutive equation for the solid-fluid relative velocity $\mathbf{v}_\mathrm{r}$. The well-known sedimentation theory due to KYNCH [30] corresponds here to the constitutive assumption

$$\mathbf{v}_\mathrm{r} = \frac{f_\mathrm{bk}(\phi)}{\phi(1-\phi)}\mathbf{k}, \tag{5}$$

where $f_\mathrm{bk}(\phi)$ is the KYNCH batch flux density function and $\mathbf{k}$ is the upwards-pointing unit vector. A more general expression,

$$\mathbf{v}_\mathrm{r} = \frac{f_\mathrm{bk}(\phi)}{\phi(1-\phi)}\left(\mathbf{k} + \frac{\sigma_\mathrm{e}'(\phi)}{\Delta \varrho g \phi}\nabla \phi\right), \tag{6}$$

has been developed in the phenomenological model of sedimentation-consolidation processes [13], in which compression effects are modeled by an effective solid stress function $\sigma_\mathrm{e}(\phi)$. The constants $\Delta\varrho > 0$ and g denote the solid-liquid mass density difference and the acceleration of gravity, respectively. It should be pointed out that the modeling performed in [13] also includes the solid and fluid component linear momentum balances, and that equation (6) represents one of these linear momentum balances after deleting advective acceleration terms, which in turn is justified by a dimensional analysis. The second linear momentum balance yields the linear momentum balance of the mixture. If all viscous and advective acceleration terms are deleted from this balance, we obtain

$$\nabla p_\mathrm{e} = -\nabla \sigma_\mathrm{e}(\phi) - \Delta \varrho g \phi \mathbf{k}, \tag{7}$$

where p_e is the effective solid stress of the mixture. We emphasize that the field equations (3), (4) and (7) together with the constitutive equation (6) are in general not sufficient to calculate the unknown fields ϕ, p_e and $\mathbf{q}$, since the volume average velocity $\mathbf{q}$ no longer occurs in the linear momentum balance of the mixture. For this reason, the viscous and advective acceleration terms have *not* been deleted in

[13] from the momentum balance of the mixture, although the dimensional analysis has at the same time shown that these terms can be expected to be small. In this paper, we demonstrate that solutions to (3), (4) and (7) do exist for closed vessels. Nevertheless, we also illustrate that the use of equation (7) has severe consequences on the choice of boundary conditions, and that these boundary conditions affect the entire flow field.

2 Derivation of the initial-boundary value problems

2.1 Properties of the constitutive functions

The model functions $f_{\rm bk}(\phi)$ and $\sigma_{\rm e}(\phi)$ involved are usually assumed to satisfy

$$f_{\rm bk}(\phi) = 0 \text{ for } \phi \leq 0 \text{ or } \phi \geq \phi_{\max},\ f_{\rm bk}(\phi) < 0 \text{ for } 0 < \phi < \phi_{\max} \tag{8}$$

and

$$\sigma_{\rm e}'(\phi) = \frac{d\sigma_{\rm e}}{d\phi} \begin{cases} = 0 & \text{for } \phi \leq \phi_{\rm c}, \\ > 0 & \text{for } \phi > \phi_{\rm c}, \end{cases} \tag{9}$$

where $\phi_{\rm c}$ is the critical concentration (or gel point) at which the solid flocs touch each other and $0 < \phi_{\max} \leq 1$ is the maximum solids concentration. Typical choices of these constitutive functions include MICHAELS and BOLGER's [36] modification

$$f_{\rm bk}(\phi) = u_\infty \phi \big(1 - (\phi/\phi_{\max})\big)^n, \quad u_\infty < 0, \quad n > 1 \tag{10}$$

of the well-known RICHARDSON and ZAKI formula [43], and the power law

$$\sigma_{\rm e}(\phi) = 0 \text{ for } \phi \leq \phi_{\rm c}, \quad \sigma_{\rm e}(\phi) = \sigma_0 \big((\phi/\phi_{\rm c})^k - 1\big), \quad \sigma_0 > 0, \quad k > 1 \text{ for } \phi > \phi_{\rm c}, \tag{11}$$

see e.g. LANDMAN and WHITE [31]. In the numerical examples presented in § 4 in this paper, we utilize the the model functions

$$f_{\rm bk}(\phi) = \begin{cases} -1.9802137 \times 10^{-4} \phi \big(1 - (\phi/0.3)\big)^{5.647}\,[\mathrm{m/s}] & \text{for } 0 \leq \phi < 0.18, \\ -5.517 \times 10^{-13} \phi^{-7.47}\,[\mathrm{m/s}] & \text{for } 0.18 \leq \phi \leq 0.3, \\ 0 & \text{otherwise} \end{cases} \tag{12}$$

and $\sigma_{\rm e}(\phi)$ given by (11) with the parameters

$$\sigma_0 = 5.7\,[\mathrm{Pa}], \quad \phi_{\rm c} = 0.1, \quad k = 9.09 \tag{13}$$

which have been determined for a calcium carbonate suspension, see [8, 15, 16]. These functions are plotted in Figure 1 together with the diffusion coefficient

$$a(\phi) = -f_{\rm bk}(\phi)\sigma_{\rm e}'(\phi)/(\Delta\varrho g \phi).$$

For alternative choices of the functions $f_{\rm bk}(\phi)$ and $\sigma_{\rm e}(\phi)$ describing the settling behaviour of real materials we refer to BÜRGER et al. [8] and GARRIDO et al. [20].

Finally, we point out that the expression (6) includes, of course, equation (5) if we set $\sigma_{\rm e} \equiv 0$, that is formally $\phi_{\rm c} = \phi_{\max}$.

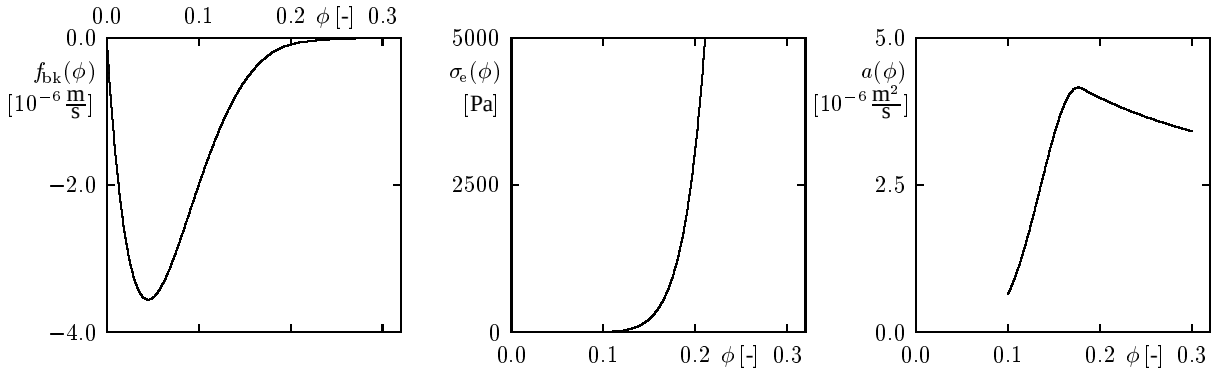

Figure 1: The model functions $f_{\mathrm{bk}}(\phi)$ (left), $\sigma_{\mathrm{e}}(\phi)$ (middle) and the resulting diffusion coefficient $a(\phi)$ (right) determined for a calcium carbonate suspension.

2.2 Properties of the field equations

We recall some properties of the field equations (3), (4) and (7). First note that due to the assumptions (8) and (9), equation (3) is of first-order hyperbolic type where $\phi \leq \phi_{\mathrm{c}}$ or $\phi = \phi_{\max}$ and of second-order parabolic type where $\phi_{\mathrm{c}} < \phi < \phi_{\max}$. In a settling column, $\phi = \phi_{\mathrm{c}}$ denotes the sediment-suspension interface. In contrast to what is known for KYNCH's theory, the location of this interface can in general not be determined a priori.

We assume that all fields depend on the Cartesian coordinates x, y, z and on time $t \geq 0$, and that z is the coordinate in direction of $\mathbf{k}$. As stated by SCHNEIDER [46], who postulated a similarly simplified mixture momentum balance, equation (7) has a remarkable consequence: Taking the curl, we get

$$\phi = \phi(z, t), \tag{14}$$

i.e. concentration varies only with height. Now we use this fact in order to formulate the field equations in their final form:

a) Condition (14) replaces the linear momentum balance (7).

b) We can rewrite $\phi \mathbf{v}_{\mathrm{s}}$ as

$$\phi \mathbf{v}_{\mathrm{s}} = \phi \mathbf{q} + f_{\mathrm{bk}}(\phi)\mathbf{k} - \nabla A(\phi), \quad A(\phi) = \int_0^{\phi} a(s)\, ds, \tag{15}$$

in order to simplify the continuity equation and to introduce the different types of boundary conditions. Equation (15) replaces the constitutive equation (6).

However, since $\mathbf{k}$ is the upwards pointing unit vector and $\phi = \phi(z, t)$, we may recast (15) into its final form

$$\phi \mathbf{v}_{\mathrm{s}} = \phi \mathbf{q} + \left(f_{\mathrm{bk}}(\phi) - \frac{\partial A(\phi)}{\partial z} \right) \mathbf{k}. \tag{16}$$

c) Equation (4) is rewritten in the form

$$\frac{\partial q_z}{\partial z} = -\left(\frac{\partial q_x}{\partial x} + \frac{\partial q_y}{\partial y}\right). \tag{17}$$

d) We replace the solid flux $\phi \mathbf{v}_\mathrm{s}$ in the continuity equation (3) by the expression (16). Using (14) and (17), we obtain the following essential simplification of the continuity equation:

$$\frac{\partial \phi}{\partial t} + \big(q_z + f'_{\mathrm{bk}}(\phi)\big)\frac{\partial \phi}{\partial z} = \frac{\partial^2}{\partial z^2}\big(A(\phi)\big). \tag{18}$$

e) We may solve (18) with respect to q_z wherever $\partial\phi/\partial z \neq 0$ and use (14) in order to conclude that

$$q_z = q_z(z,t). \tag{19}$$

We must assume this equation also wherever $\partial\phi/\partial z = 0$ in order to obtain solutions that are stable with respect to small perturbations of the concentration field, see SCHNEIDER [46].

Equations (14) to (19) provide all information about the three-dimensional field equations introduced in § 1. The properties which we have established here were studied by SCHNEIDER [46] for the special case $a(\phi) \equiv 0$ corresponding to KYNCH's theory.

2.3 Boundary conditions

We consider the boundary conditions for a closed vessel $\Omega \subset \mathbb{R}^3$ and a general solution of the field equations derived before. A particular geometry of the vessel will not yet be specified.

Let $\mathbf{n} = (n_x, n_y, n_z)^{\mathrm{T}}$ be a vector which points into the vessel and is orthogonal to its boundary. Since the boundary is assumed to be impermeable for the solid and the fluid, the boundary conditions

$$(\phi \mathbf{v}_\mathrm{s}) \cdot \mathbf{n} = 0, \tag{20}$$

$$\big((1-\phi)\mathbf{v}_\mathrm{f}\big) \cdot \mathbf{n} = 0 \tag{21}$$

should be satisfied simultaneously at any boundary point of the vessel. Equation (2) may be used in order to rewrite these conditions in terms of $\mathbf{q}$ and $\mathbf{v}_\mathrm{s}$ as

$$(\phi \mathbf{v}_\mathrm{s}) \cdot \mathbf{n} = 0, \quad \mathbf{q} \cdot \mathbf{n} = 0\,. \tag{22}$$

We restrict ourselves to sedimentation vessels for which $n_z \neq 0$ for every normal vector $\mathbf{n}$ of the boundary. This assumption includes for example conical tanks or

any other vessel with inclined walls which are not parallel to the z-axis. Then equations (16) and (22) immediately imply

$$\left(f_{\mathrm{bk}}(\phi) - \frac{\partial A(\phi)}{\partial z} \right)(z,t) = 0 \ \text{ for every height } z,\ t > 0. \tag{23}$$

First note that (23) only describes a stationary flow, since this equation may also be obtained by setting $\mathbf{v}_{\mathrm{s}} = \mathbf{q} = 0$ in (16). This is a very strange implication, because we started with a flow field that is not stationary in general. While for $a(\phi) \not\equiv 0$, (23) may possess non-trivial solutions (but reduces to $\phi = 0$ wherever $\phi \le \phi_{\mathrm{c}}$), this equation implies for $a(\phi) \equiv 0$ (corresponding to KYNCH's theory) in view of the assumption (8) that $\phi = 0$ or $\phi = \phi_{\max}$ for any z. Furthermore, it should be emphasized that equation (23) follows only from very general assumptions on the form of the vessel and the conditions for impermeable boundaries, but *not* from assumptions on the dynamics of the flow fields.

We conclude that it is impossible to require both boundary conditions in (22) simultaneously for every non-vertical wall. To define appropriate boundary conditions, we now distinguish between upward-facing and downward-facing walls. We assume that the domain $\Omega \subset \mathbb{R}^3$ has a smooth boundary $\Gamma = \partial\Omega$, and define the upwards-facing and downwards-facing parts of Γ, Γ_{u} and Γ_{d}, by

$$\Gamma_{\mathrm{u}} = \big\{(x,y,z) \in \Gamma : \mathbf{n}(x,y,z) \cdot \mathbf{k} > 0\big\}, \quad \Gamma_{\mathrm{d}} = \big\{(x,y,z) \in \Gamma : \mathbf{n}(x,y,z) \cdot \mathbf{k} < 0\big\}. \tag{24}$$

Since we wish to admit a thin boundary layer of clear liquid beneath downward-facing walls, we assume that there only the normal component of $\phi\mathbf{v}_{\mathrm{s}}$ vanishes, i.e.

$$\big(\phi\mathbf{v}_{\mathrm{s}}\big) \cdot \mathbf{n} = 0 \text{ on } \Gamma_{\mathrm{d}}. \tag{25}$$

There are two alternative ways to formulate boundary conditions for upward-facing walls. From a rigorous point of view, one should assume that the upward-facing walls are impermeable to the solid phases, that is, we prescribe

$$\big(\phi\mathbf{v}_{\mathrm{s}}\big) \cdot \mathbf{n} = 0 \text{ on } \Gamma_{\mathrm{u}}. \tag{26}$$

This formulation excludes the formation of any thin solid boundary layer on upward-facing inclined walls, which are not consistent with the condition (14).

On the other hand, we may admit the formation of a small boundary layer of sediment on upward-facing walls. To motivate this assumption, consider a configuration with two parallel inclined walls as a prototype of the inclined settling vessel producing the Boycott effect. The existence of a boundary layer of upwards streaming liquid beneath the downward-facing inclined must be compensated by an accelerated sedimentation rate of the bulk suspension as compared to a vertical vessel. However, we shall see that imposing the boundary condition (26) will lead to exactly

the same concentration profiles as in a vertical column. We therefore consider as an alternative formulation the boundary condition

$$\mathbf{q} \cdot \mathbf{n} = 0 \text{ on } \Gamma_{\mathrm{u}}, \tag{27}$$

i.e. allow that material may leave the boundary and form a boundary layer of mixture. It should be pointed out that (27) is similar to SCHNEIDER's formulation [46]. However, he imposed this condition not exactly on the rigid boundary, but on the sediment-suspension interface. In the case of KYNCH's theory, i.e. in the absence of effective solid stress, and if the initial concentration is sufficiently small, all sediment layers will have the same solid concentration $\phi_{\max}$. The location of the sediment-suspension interface can then indeed be predicted a priori. This is not the case with the constitutive equation (6). For this reason, we assume a priori that the thickness of the boundary layer is small and impose the boundary condition (27) on the rigid wall.

In the sequel and in the examples studied, both types of boundary conditions (26) and (27) will be considered. We point out that the choice between (26) and (27), motivated by the assumption of a sediment boundary layer, appears to affect the flow only locally, i.e. near the vicinity of the upward-facing wall. We shall see that this not the case. In fact, the assumption of boundary layers near both types of walls will severely affect the global flow field in the entire vessel. A final discussion of these consequences is presented in § 5.

In the sequel, we consider exclusively two-dimensional or axisymmetric flows in tanks with flat top or bottom and emphasize that the case of vessels having downward-facing walls enhancing the sedimentation rate is of particular interest to applications. Therefore we shall not discuss all possible combinations of downward- and upward-facing walls, and impose on the latter either boundary condition (26) or (27), but limit ourselves to vessels having at least one downward-facing wall. Consequently, there are essentially three different cases to distinguish.

2.4 Two-dimensional model equations

We are interested in two types of solutions, namely in two-dimensional planar flows and flows which are symmetric with respect to the z-axis. In the sequel, we restrict the general field equations derived before to these types of motion.

We first consider planar flows which are constant with respect to y. Then (17) yields

$$\frac{\partial q_z}{\partial z}(z,t) = -\frac{\partial q_x}{\partial x}(x,z,t). \tag{28}$$

Integrating (28) with respect to x, we obtain

$$q_x(x,z,t) = -x\,\frac{\partial q_z}{\partial z}(z,t) + C(z,t),$$

with an unknown function $C(z,t)$. Consequently, the components of the volume-average velocity $\mathbf{q}$ read

$$q_x = -x \cdot \frac{\partial q_z}{\partial z}(z,t) + C(z,t), \quad q_y = q_y(x,z,t), \quad q_z = q_z(z,t). \tag{29}$$

For the flows considered here, the field q_y may be chosen arbitrarily. This component will not appear in the formulation of the boundary conditions since these are formulated in terms of the normal components of $\mathbf{q}$ and $\mathbf{v}_s$.

Next we consider flows which are symmetric with respect to the z-axis. The height variable is z and the horizontal or radial variable is r. We replace the Cartesian coordinates by cylindrical coordinates given by $x = r\cos\theta$ and $y = r\sin\theta$. The assumption of axisymmetry implies that $\mathbf{q}$ depends on r, θ, z and t in the following form, where have inserted (19):

$$q_x(x,y,z,t) = \hat{q}(r,z,t)\cos\theta, \quad q_y(x,y,z,t) = \hat{q}(r,z,t)\sin\theta, \quad q_z(x,y,z,t) = q_z(z,t). \tag{30}$$

Of the equations (14) to (19), only (17) takes a different form in cylindrical axisymmetric case, namely it now reads

$$\frac{\partial q_z}{\partial z}(z,t) = -\frac{1}{r}\frac{\partial (r\hat{q})}{\partial r}(r,z,t). \tag{31}$$

Multiplying (31) with r and integrating with respect to r, we obtain

$$r\hat{q}(r,z,t) = -\frac{r^2}{2}\frac{\partial q_z}{\partial z}(z,t) + \hat{C}(z,t)$$

with a suitable function $\hat{C} = \hat{C}(z,t)$. We set $r = 0$ and note that r is independent of z and t in order to conclude that $\hat{C} \equiv 0$, i.e. we obtain

$$\hat{q}(r,z,t) = -\frac{r}{2}\frac{\partial q_z}{\partial z}(z,t). \tag{32}$$

The final result may be summarized as

$$q_x = -\frac{x}{2}\frac{\partial q_z}{\partial z}(z,t), \quad q_y = -\frac{y}{2}\frac{\partial q_z}{\partial z}(z,t), \quad q_z = q_z(z,t). \tag{33}$$

These equations for axisymmetric flows are the analogue of (29) for planar flows. However, in the planar case the function $C(z,t)$ does in general not vanish, since it is necessary to describe settling processes in unsymmetric tanks (e.g. with parallel inclined walls).

2.5 Final form of the governing equations for two-dimensional flows

We now specify boundary conditions for the two-dimensional flows proposed in § 2.4. The final result will be a coupled system of one ordinary and one partial differential equation for the two scalar fields $\phi(z,t)$ and $q_z(z,t)$.

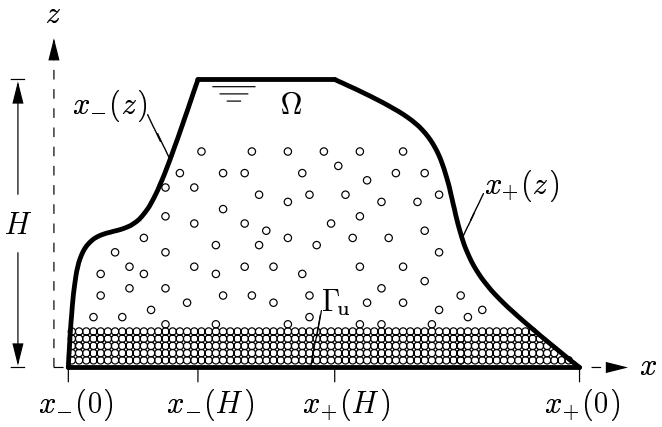

Figure 2: Cross-section of a two-dimensional sedimentation vessel with curvilinear boundaries.

First, we consider planar flows which are constant with respect to y and a vessel with a flat top $z = H$ and a flat bottom $z = 0$ having two curvilinear boundaries $x_-(z)$ and $x_+(z)$, $0 \leq z \leq H$, see Figure 2. The conditions corresponding to these boundaries will now be employed in order to derive the abovementioned system, which, of course, will depend on the particular geometry of the vessel.

We now determine a complete set of equations for the unknowns $\phi(z,t)$, $q_z(z,t)$ and $C(z,t)$. To this end, we first consider the boundary condition (25). In view of equation (16) and the representation (29) of the volume-average velocity field $\mathbf{q}$ for planar flows, we may rewrite the components of $\mathbf{v}_\mathrm{s}$ as

$$v_{\mathrm{s}x} = -x \cdot \frac{\partial q_z}{\partial z}(z,t) + C(z,t), \quad v_{\mathrm{s}y} = q_y(x,z,t), \quad v_{\mathrm{s}z} = q_z(z,t) + \frac{1}{\phi}\left(f_{\mathrm{bk}}(\phi) - \frac{\partial A(\phi)}{\partial z}\right). \tag{34}$$

Obviously, orthogonal vectors to the two curved boundaries are given by

$$\mathbf{n}_\pm(z) = \pm\big(-1, 0, x'_\pm(z)\big)^{\mathrm{T}}. \tag{35}$$

Without loss of generality, we may assume that $x_-(z)$ is a downward-facing wall, i.e. we have

$$\big(\phi(z,t)\mathbf{v}_\mathrm{s}(x_-(z),z,t)\big) \cdot \mathbf{n}_-(z) = 0. \tag{36}$$

Inserting the representation (34) of $\mathbf{v}_\mathrm{s}$, where we set $x = x_-(z)$, and (35) into the boundary condition (36), we obtain

$$C(z,t) = x_-(z)\frac{\partial q_z}{\partial z}(z,t) + x'_-(z)\left[q_z(z,t) + \frac{1}{\phi(z,t)}\left(f_{\mathrm{bk}}\big(\phi(z,t)\big) - \frac{\partial A(\phi)}{\partial z}(z,t)\right)\right]. \tag{37}$$

To proceed with the derivation of the model equations, we distinguish two cases. First, we assume that $x_+(z)$ is another downward-facing wall, or that $x_+(z)$ is an upward-facing wall on which the boundary condition (26) are prescribed (this includes the case of an axisymmetric vessel), and second, we assume that $x_+(z)$ is an upward-facing wall where boundary condition (27) is imposed.

1. In the first case, the condition $\big(\phi(z,t)\mathbf{v}_{\mathrm{s}}(x_+(z),z,t)\big)\cdot\mathbf{n}_+(z)=0$ is valid. In an analogous way to the derivation of (37), we obtain

$$C(z,t)=x_+(z)\frac{\partial q_z}{\partial z}(z,t)+x_+'(z)\left[q_z(z,t)+\frac{1}{\phi(z,t)}\left(f_{\mathrm{bk}}\big(\phi(z,t)\big)-\frac{\partial A(\phi)}{\partial z}(z,t)\right)\right]. \tag{38}$$

Adding equations (37) and (38), we see that $C(z,t)=0$ wherever $x_-(z)=-x_+(z)$; in particular, $C\equiv 0$ for a vessel which is symmetric with respect to $x=0$. Subtracting (37) from (38), we obtain the following ordinary differential equation for $q_z(z,t)$:

$$\frac{\partial q_z}{\partial z}+\frac{x_+'(z)-x_-'(z)}{x_+(z)-x_-(z)}\left[q_z+\frac{1}{\phi}\left(f_{\mathrm{bk}}\big(\phi\big)-\frac{\partial A(\phi)}{\partial z}\right)\right]=0. \tag{39}$$

Taking into account the continuity equation (18), we thus obtain a system of a first-order ordinary differential equation (with respect to z) coupled to a hyperbolic-parabolic degenerate quasilinear partial differential equation for the two unknown fields $\phi(z,t)$ and $q_z(z,t)$.

For a flow which is axisymmetric with respect to the z-axis, we can only prescribe a radius function $r=r(z)$ with $0\le z\le H$ and a single boundary condition that does not depend on θ. Using equation (16) and the representation (33) of $\mathbf{q}$ for axisymmetric flows, we obtain

$$v_{\mathrm{s}x}=-\frac{r}{2}\frac{\partial q_z}{\partial z}(z,t)\cos\theta, \tag{40a}$$

$$v_{\mathrm{s}y}=-\frac{r}{2}\frac{\partial q_z}{\partial z}(z,t)\sin\theta, \tag{40b}$$

$$v_{\mathrm{s}z}=q_z(z,t)+\frac{1}{\phi}\left(f_{\mathrm{bk}}(\phi)-\frac{\partial A(\phi)}{\partial z}\right). \tag{40c}$$

For $\theta=0$, the vector $\mathbf{n}(z)=\big(-1,0,r'(z)\big)^{\mathrm{T}}$ is orthogonal to the inclined boundaries of the symmetric vessel. As before we use the boundary condition (25) and obtain

$$\frac{\partial q_z}{\partial z}+\frac{2r'(z)}{r(z)}\left[q_z+\frac{1}{\phi}\left(f_{\mathrm{bk}}(\phi)-\frac{\partial A(\phi)}{\partial z}\right)\right]=0. \tag{41}$$

Of course, equation (41) is also coupled to equation (18). To rewrite the coupled system for $q_z(z,t)$ and $\phi(z,t)$ in a uniform manner for both the planar

and the axisymmetric case, we introduce the parameter σ and the function $d(z)$ by

$$d(z) = x_+(z) - x_-(z), \quad \sigma = 1 \qquad \text{for planar flows,} \tag{42}$$

$$d(z) = 2r(z), \quad \sigma = 2 \qquad \text{for axisymmetric flows.} \tag{43}$$

Then we obtain

$$\frac{\partial q_z}{\partial z} + \frac{\sigma d'(z)}{d(z)} q_z = -\frac{\sigma d'(z)}{d(z)\phi} \left(f_{\mathrm{bk}}(\phi) - \frac{\partial A(\phi)}{\partial z} \right), \tag{44}$$

$$\frac{\partial \phi}{\partial t} + \big(q_z + f'_{\mathrm{bk}}(\phi)\big) \frac{\partial \phi}{\partial z} = \frac{\partial^2 A(\phi)}{\partial z^2}. \tag{45}$$

2. If the boundary $x_+(z)$ is an upward-facing wall on which the boundary condition (27), which reads here $\mathbf{q} \cdot \mathbf{n}_+(z) = 0$, we obtain in view of (29)

$$C(z,t) = x_+(z) \frac{\partial q_z}{\partial z} + x'_+(z) q_z. \tag{46}$$

The right-hand parts of (37) and (46) must be equal. This yields the following ordinary differential equation for q_z, where $d(z)$ is defined as in (42):

$$\frac{\partial q_z}{\partial z} + \frac{d'(z)}{d(z)} q_z = \frac{x'_-(z)}{d(z)\phi} \left(f_{\mathrm{bk}}(\phi) - \frac{\partial A(\phi)}{\partial z} \right). \tag{47}$$

This equation is again coupled with (18), i.e. we obtain the coupled system (47), (45) instead of (44), (45).

Now we have to formulate initial conditions and boundary conditions corresponding to the flat top and bottom for this system. The initial condition is

$$\phi(z,0) = \phi_0(z), \quad 0 \le \phi_0(z) \le \phi_{\max} \quad \text{for } 0 \le z \le H. \tag{48}$$

Moreover we prescribe the boundary conditions

$$q_z(0,t) = 0, \tag{49}$$

$$\phi(H,t) = 0. \tag{50}$$

Finally, we require that neither fluid nor solid passes through the horizontal boundary $z = 0$, and prescribe

$$\left(f_{\mathrm{bk}}(\phi) - \frac{\partial A(\phi)}{\partial z} \right)(0,t) = 0. \tag{51}$$

In the case of presence of an upward-facing wall on which sediment may accumulate, we assume that there is no downwards creeping flow of the solid material.

Of course, once we have calculated the fields $\phi(z,t)$ and $q_z(z,t)$ from the system (44), (45), we immediately obtain $\mathbf{q}$ and $\mathbf{v}_{\mathrm{s}}$ from (29), (34) and (37) in the planar and from (33), (37) and (40) in the axisymmetric case.

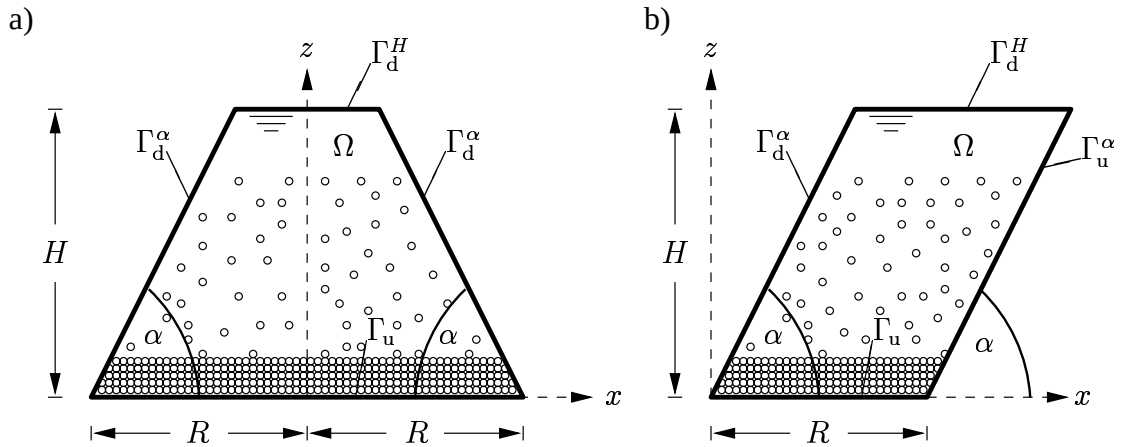

Figure 3: Batch settling in a vessel a) with inclined or conical walls, b) with parallel inclined walls.

An immediate consequence of the coupling between the field q_z and the concentration distribution ϕ expressed in both systems (44), (45) and (47), (45) is that an initial concentration distribution ϕ_0 and the initial volume average velocity field $\mathbf{q}(x, z, 0)$ cannot be prescribed independently. Rather, only ϕ_0 can be prescribed, and the instantaneous velocity field $\mathbf{q}(x, z, 0)$ is determined by inserting ϕ_0 into the right-hand part of equation (44) or equation (47) and integrating the respective equation with respect to z using the boundary condition (49).

3 Sedimentation in vessels with inclined plane or conical walls

3.1 Sedimentation in roof-shaped or conical vessels

Here we evaluate two explicit examples, namely for a planar flow in a roof-shaped vessel and a flow symmetric with respect to the z-axis in a conical vessel. In both cases we provide a vessel with a flat bottom of width $2R$, height H and side wall inclination angle $0 < \alpha < \pi/2$, see Figure 3a).

In the first case of a planar flow with $\sigma = 1$ we set

$$x_+(z) = R - z\cot\alpha;\ x_-(z) = -x_+(z);\ d(z) = 2(R - z\cot\alpha) \tag{52}$$

and note that $C \equiv 0$. In the second case with $\sigma = 2$ we obtain

$$r(z) = R - z\cot\alpha;\ d(z) = 2(R - z\cot\alpha). \tag{53}$$

Then we can use (44) for both cases with the same function $d(z)$ and obtain the following equation for q_z:

$$\frac{\partial q_z}{\partial z} - \frac{\sigma\cot\alpha}{R - z\,\cot\alpha}\cdot q_z = \frac{\sigma\cot\alpha}{R - z\,\cot\alpha}\cdot\frac{1}{\phi}\left(f_{\mathrm{bk}}(\phi) - \frac{\partial A(\phi)}{\partial z}\right). \tag{54}$$

In the sequel we will exclusively consider a constant initial concentration in order to solve the initial-boundary value problem (44)–(51), i.e. (48) is replaced by

$$\phi(z,0) = \phi_0 = \text{constant}, \quad 0 < \phi_0 < \phi_{\max}. \tag{55}$$

Equation (54) may be solved explicitly for a constant concentration $\phi_* < \phi_c$ which does not depend on z and t for some region in space and time. In this case we obtain the solution

$$q_z(z,t) = \frac{\kappa(t)}{d^\sigma(z)} - \frac{f_{bk}(\phi_*)}{\phi_*}\,, \tag{56}$$

where $\kappa(t)$ is in general a time-dependent function. Now we discuss the implications of formula (56) for two special cases, namely for a very small initial time $t \to 0$ and for $t \to \infty$ with a final consolidation state. In the case $t \to 0$ we use the initial condition $\phi(0,x) = \phi_0$, the boundary condition $q_z(0,t) = 0$ and obtain

$$q_x(x,z,0) = -\frac{x}{R}\,\frac{f_{bk}(\phi_0)}{\phi_0}\,\frac{\cot\alpha}{\left(1-\frac{z}{R}\cot\alpha\right)^{\sigma+1}}\,,\ q_z(z,0) = \frac{f_{bk}(\phi_0)}{\phi_0}\left(\frac{1}{\left(1-\frac{z}{R}\cot\alpha\right)^{\sigma}} - 1\right)\,. \tag{57}$$

There results the following initial velocity field $\mathbf{v}_s$

$$v_{sx}(x,z,0) = -\frac{x}{R}\,\frac{f_{bk}(\phi_0)}{\phi_0}\,\frac{\cot\alpha}{\left(1-\frac{z}{R}\cot\alpha\right)^{\sigma+1}}\,,\ v_{sz}(z,0) = \frac{f_{bk}(\phi_0)}{\phi_0}\left(1-\frac{z}{R}\cot\alpha\right)^{-\sigma}\,. \tag{58}$$

If we enlarge the diameter R of the vessel for fixed height H and set for example $x = R/2$, we obtain for $0 < z < H$

$$\lim_{R\to\infty} v_{sx}(R/2,z,0) = -\frac{f_{bk}(\phi_0)}{2\phi_0}\cot\alpha\,.$$

However, we expect that for $R \to \infty$ the influence of the boundaries should decay, i.e. that

$$\lim_{R\to\infty} v_{sx}(R/2,z,0) = 0. \tag{59}$$

This is a clear contradiction to equation (58), which indicates the initial velocity fields are not physically correct in the entire vessel and not only in the vicinity of boundary layers.

In order to describe the final consolidation state for $t \to \infty$ we restrict ourselves to KYNCH's theory, i.e. the case considered by SCHNEIDER [46], and set

$$A(\phi) \equiv a(\phi) \equiv 0. \tag{60}$$

Here we expect a sediment layer of height z_c with $0 < z_c < H$ and constant concentration $\phi = \phi_{\max}$ for $0 \le z \le z_c$, and a clear liquid zone with $\phi = 0$ for $z_c < z \le H$.

We consider a flux density function $f_{\rm bk}(\phi)$ that satisfies (8) and use the boundary condition (49) to conclude from (56) that $q_z \equiv 0$ in the sediment-layer. Formula (56) predicts a strange behaviour in the stationary clear liquid region. In the stationary case, we may replace $\kappa(t)$ by some constant κ_0. Taking into account that $q_z \equiv 0$ in the sediment layer and that

$$\lim_{\phi_* \to 0} f_{\rm bk}(\phi_*)/\phi_* = u_\infty, \tag{61}$$

we obtain

$$q_z(z) = u_\infty \left((d^\sigma(z_{\rm c})/d^\sigma(z)) - 1 \right) < 0 \ \text{ for } z > z_{\rm c}. \tag{62}$$

Consequently, $q_z(z)$ cannot vanish in the clear liquid zone for the final consolidation state since the vessel has the variable cross-section $d(z) = 2(R - z\cot\alpha)$. In particular, (62) implies that $q_z(H) < 0$, i.e. even in the stationary final state a positive amount of clear liquid per unit time leaves the vessel through the inclined walls and returns into the vessel through the upper boundary. Once again the initial velocity fields are not physically correct in the whole vessel and not only in the vicinity of boundary layers.

3.2 Sedimentation between inclined parallel walls

We consider a two-dimensional sedimentation vessel with two parallel inclined walls, see Figure 3b). In this case, we have

$$\sigma = 1;\ x_+(z) = R + z\cot\alpha;\ x_-(z) = z\cot\alpha;\ d(z) = R. \tag{63}$$

As in § 2.5, we have to analyze each case of boundary condition either (26) or (27) on $x_+(z)$ separately.

1. If we prescribe boundary conditions (26), we immediately obtain from (44)

$$\frac{\partial q_z}{\partial z} \equiv 0. \tag{64}$$

From the boundary condition (49) we conclude that q_z vanishes identically. In this case, only the scalar degenerate hyperbolic-parabolic equation

$$\frac{\partial \phi}{\partial t} + \frac{\partial}{\partial z}\left(f_{\rm bk}(\phi) - \frac{\partial A(\phi)}{\partial z} \right) = 0, \tag{65}$$

which is independent of the inclination angle α, has to be solved. This means that the concentration profiles are exactly the same as in a vertical settling column of height H, which have for example been calculated in [6, 7].

Taking into account that q_z vanishes everywhere and using (2), (34) and (37), we obtain the following solid and liquid phase velocity fields for $\phi > 0$:

$$v_{{\rm s}x} = \frac{1}{\phi}\left(f_{\rm bk}(\phi) - \frac{\partial A(\phi)}{\partial z} \right)\cot\alpha, \quad v_{{\rm s}z} = \frac{1}{\phi}\left(f_{\rm bk}(\phi) - \frac{\partial A(\phi)}{\partial z} \right), \tag{66}$$

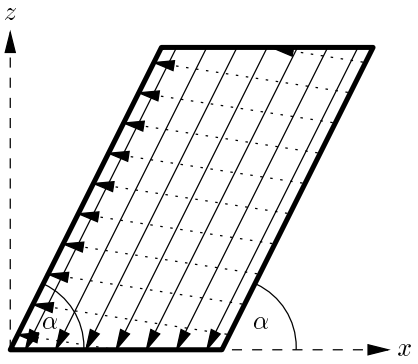

Figure 4: The flow field between two parallel inclined plates for $\phi = const.$ in the case of imposing boundary condition (26) on the upward-facing wall. The solid and dotted arrows denote the solid and fluid particle trajectories, respectively.

$$v_{\mathrm{f}x} = \frac{1}{\phi}\left(f_{\mathrm{bk}}(\phi) - \frac{\partial A(\phi)}{\partial z}\right)\cot\alpha, \quad v_{\mathrm{f}z} = -\frac{1}{1-\phi}\left(f_{\mathrm{bk}}(\phi) - \frac{\partial A(\phi)}{\partial z}\right). \quad (67)$$

Here, we have omitted the y-components, since they do not contribute to a planar flow. It should be pointed out that these expressions are also well defined for $\phi = 0$ for virtually all practically relevant flux density and effective solid stress functions $f_{\mathrm{bk}}(\phi)$ and $\sigma_{\mathrm{e}}(\phi)$, for example those given in (10) and (11).

We note that the entire solid phase velocity field is parallel to the inclined walls and therefore satisfies the prescribed boundary condition (25). In contrast, the fluid passes the inclined boundaries, which is illustrated in Figure 4, where both velocity fields are depicted in a region where the concentration takes a constant value $\phi_0 > 0$.

2. If we assume that boundary condition (27) is valid on the upward-facing wall, the coupled system (47), (45) takes the form

$$\frac{\partial q_z}{\partial z} = \frac{\cot\alpha}{R\phi}\left(f_{\mathrm{bk}}(\phi) - \frac{\partial A(\phi)}{\partial z}\right), \quad (68)$$

$$\frac{\partial \phi}{\partial z} + \left(q_z + f'_{\mathrm{bk}}(\phi)\right)\frac{\partial \phi}{\partial z} = \frac{\partial^2 A(\phi)}{\partial z^2}. \quad (69)$$

In contrast to the previous case, we now obtain a coupling between the concentration distribution ϕ and the volume average flow field $\mathbf{q}$. The solid concentration profiles will not be the same as in the one-dimensional case, and the solid phase velocity field will not be parallel to the inclined walls. In fact, we may repeat the analysis performed in § 3.1 for a sub-critical constant concentration $\phi_0 < \phi_{\mathrm{c}}$. We then obtain from (68) that

$$q_z = \frac{f_{\mathrm{bk}}(\phi_0)\cot\alpha}{\phi_0 R}\cdot z + \tilde{\kappa}(t), \quad (70)$$

From boundary condition (49) we immediately obtain that the integration constant $\tilde{\kappa}$ vanishes. Moreover, we can employ (37) to obtain

$$C(z,0) = \left(1 + \frac{2z\cot\alpha}{R}\right)\frac{f_{\mathrm{bk}}(\phi_0)\cot\alpha}{\phi_0}, \tag{71}$$

from which we get in view of (29) and (34)

$$q_x(x,z,0) = \left(1 + \frac{2z\cot\alpha - x}{R}\right)\frac{f_{\mathrm{bk}}(\phi_0)\cot\alpha}{\phi_0}, \quad q_z(z,0) = \frac{f_{\mathrm{bk}}(\phi_0)\cot\alpha}{\phi_0 R}\cdot z, \tag{72}$$

$$v_{\mathrm{s}x}(x,z,0) = \left(1 + \frac{2z\cot\alpha - x}{R}\right)\frac{f_{\mathrm{bk}}(\phi_0)\cot\alpha}{\phi_0}, \tag{73}$$

$$v_{\mathrm{s}z}(z,0) = \left(1 + \frac{z\cot\alpha}{R}\right)\frac{f_{\mathrm{bk}}(\phi_0)}{\phi_0}. \tag{74}$$

Obviously, we get from (73)

$$v_{\mathrm{s}x}(R/2,z,0) = \left(\frac{1}{2} + \frac{2z\cot\alpha}{R}\right)\frac{f_{\mathrm{bk}}(\phi_0)\cot\alpha}{\phi_0}, \tag{75}$$

and hence

$$\lim_{R\to\infty} v_{\mathrm{s}x}(R/2,z,0) = f_{\mathrm{bk}}(\phi_0)\cot\alpha/(2\phi_0). \tag{76}$$

As in the case of a conical vessel, we expect that the influence of the inclined boundaries vanishes for $R \to \infty$, i.e. that (59) is valid, which is a clear contradiction to (76).

As in § 3.1, we also consider the final consolidated state for $t \to \infty$, where for simplicity we restrict ourselves again to the constitutive assumption (60). The final state of the system will be a sediment layer of concentration $\phi_{\max}$ and height z_{c} with a clear liquid zone above. Using a flux density function $f_{\mathrm{bk}}(\phi)$ that satisfies (8), we may again conclude from (49) that $q_z \equiv 0$ for $z \le z_{\mathrm{c}}$. In view of (61), we obtain

$$q_z(z) = u_\infty \cot\alpha/R < 0 \quad \text{for } z > z_{\mathrm{c}}, \tag{77}$$

hence, as in the case of a conical vessel, the model predicts that even in a final, stationary state a positive amount of liquid leaves the vessel through the inclined wall and returns into the tank through the upper boundary. Clearly, this phenomenon is not restricted to the vicinity of the boundary.

4 Numerical examples

The following solution procedure has been implemented in order to obtain transient solutions of the initial-boundary value problems consisting of the field equations (44)

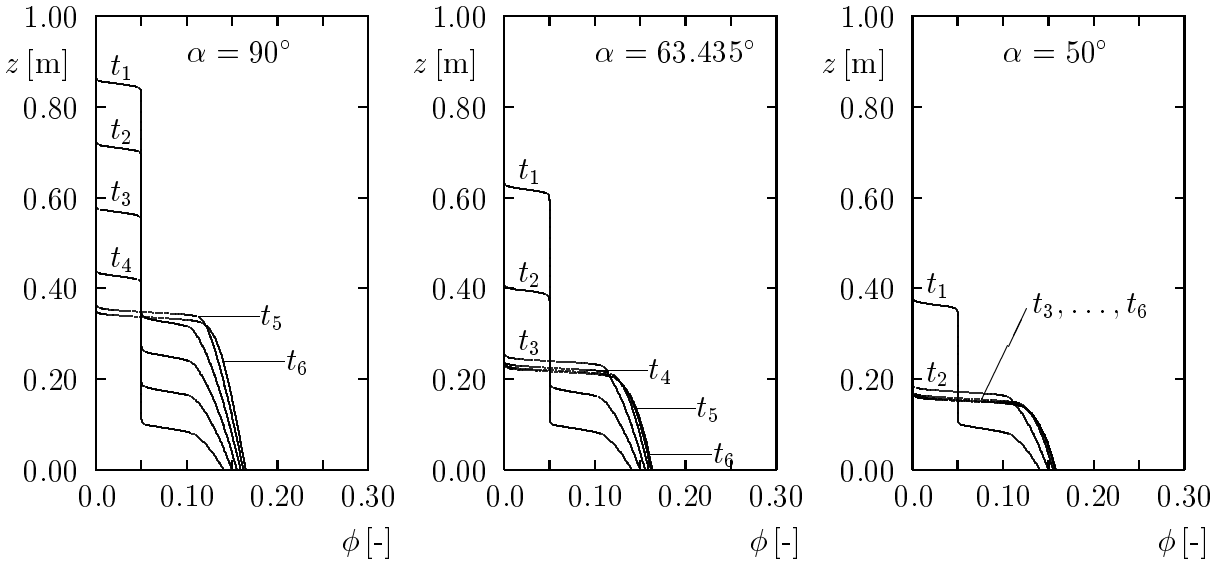

Figure 5: Simulated concentration profiles at $t_i = 2000i\,[\mathrm{s}]$, $i = 1, \ldots, 6$, in a cylindrical sedimentation vessel (left) and in conical vessels with wall inclination angles $\alpha = 63.425°$ (middle) and $\alpha = 50°$ (right).

(or (47)) and (45) and the initial and boundary conditions (48)–(51): Assume that a time step $\Delta t > 0$ is given, and that $t_n = n\Delta t$, $n = 0, 1, 2, \ldots, N$. We then use the following steps alternately:

1. Assume that $\phi(\cdot, t_n)$ is given (from the previous step or by the initial condition for $n = 0$). Then calculate $q_z(\cdot, t_{n+1})$ by inserting $\phi(\cdot, t_n)$ into the right-hand part of equation (44) (or equation (47)) and integrating this equation with respect to z using the boundary condition $q_z(0, t_{n+1}) = 0$.

2. Replace q_z in equation (45) by $q_z(\cdot, t_{n+1})$. Then calculate $\phi(\cdot, t_{n+1})$ from $\phi(\cdot, t_n)$ by using the PDE (45), the boundary conditions $\phi(H, t) = 0$ and (51).

In our implementation, we use a polygonal method for the first step and a finite-difference operator splitting method described in detail in [14, Ch. 10]. In fact, there exists a variety of discretizations suitable for equation (45), see [10, 11] for an overview. One can either use monotone finite difference schemes with numerical fluxes that include both the convective and the diffusive part or, in an 'operator splitting' methodology, select the optimal existing methods for the convective and the diffusive part and solve both separately. We refer to [19, 25, 26] for an excellent introduction to discretization techniques for degenerate convection-diffusion equations based on operator splitting. The diffusion term $\partial^2 A(\phi)/\partial z^2$ should, however, always be discretized in a conservative manner to ensure convergence to the entropy weak solution of equation (45) together with the corresponding initial and boundary conditions.

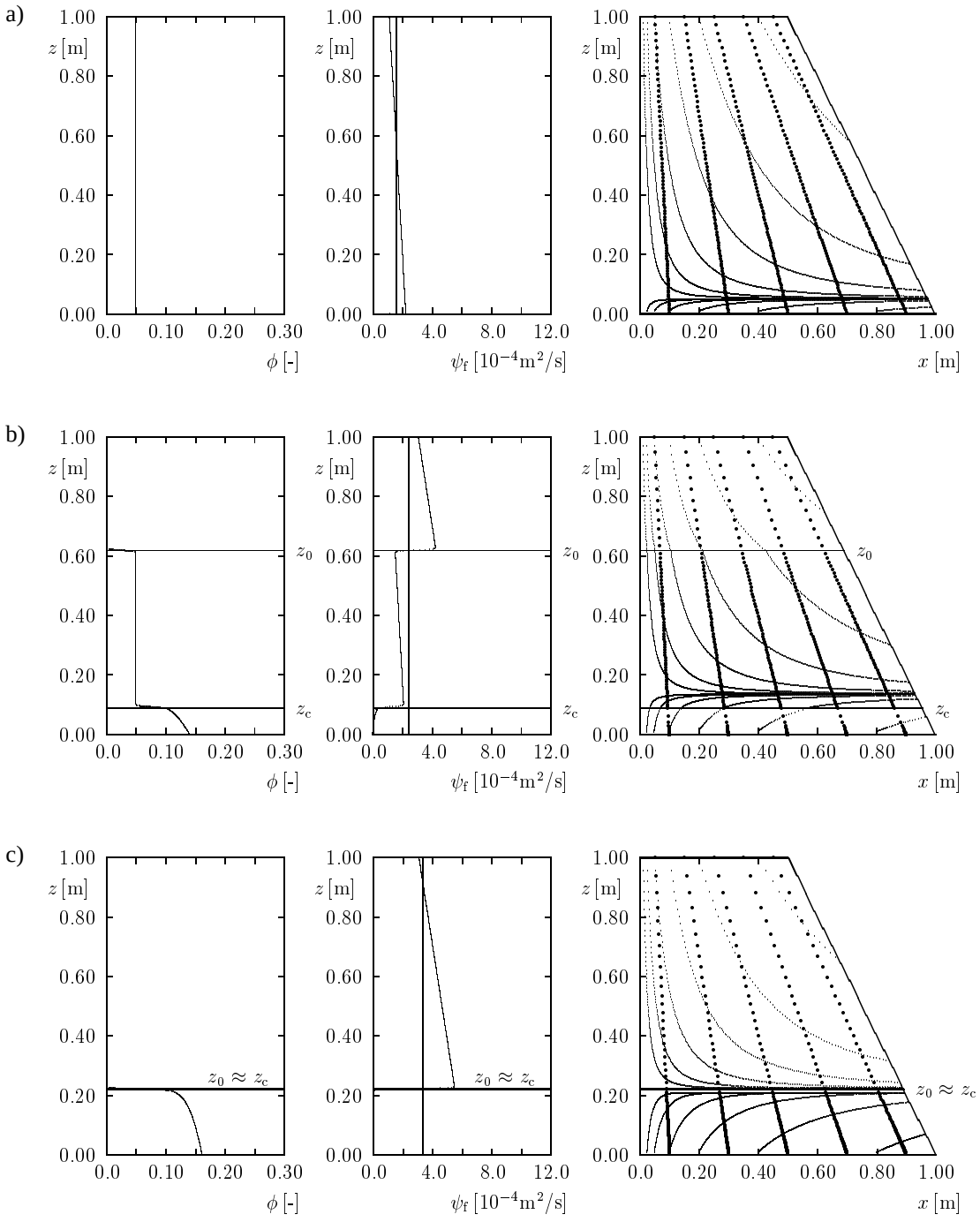

Figure 6: Simulation of sedimentation in a conical vessel with $\alpha = 63.425°$: concentration profiles (left), boundary fluid flux density (middle) and solid (fat dots) and fluid particle paths (right) at times (a) $t = 0$, (b) $t = 2000\,[\mathrm{s}]$ and (c) $t = 12000\,[\mathrm{s}]$.

To illustrate the predictions of the initial-boundary value problems, we consider the suspension whose material behaviour is defined by the model functions (11) and (12) with the parameters specified in (13), see Figure 1. Note that $a(\phi)$ not only vanishes on the interval $[0, \phi_c]$ but is even discontinuous at $\phi = \phi_c$. However, in view of recent existence and uniqueness results by BÜRGER et al. [9] for the simpler case $q_z = q_z(t)$ and the fact that discontinuous diffusion coefficients are explicitly included in the numerical schemes discussed above, this unusual feature need not cause particular difficulties.

4.1 Sedimentation in a conical vessel

We first consider an initially homogeneous suspension of concentration $\phi_0 \equiv 0.05$ in conical vessels of height $H = 1\,[\mathrm{m}]$, bottom radius $R = 1\,[\mathrm{m}]$ and different inclination angles $\alpha = 90°$, $\alpha = \arctan 2 = 63.435°$ and $\alpha = 50°$. Figure 5 shows simulated concentration profiles for $t = t_i = 2000i\,[\mathrm{s}]$, $i = 1, \ldots, 6$ in each of the three vessels. We observe that decreasing α considerably increases the settling rate, i.e. the propagation velocity (in absolute value) of the supernate-suspension interface. These concentration profiles have been calculated with a spatial accuracy of $\Delta z = L/500$.

Next, to illustrate details of the flow field, we consider the case $\alpha = \arctan 2 = 63.435°$. Figure 6 shows the numerical solution at three different times, viz. $t = 0$ (a), $t = 2000\,[\mathrm{s}]$ (b) and $t = 13000\,[\mathrm{s}]$ (c). Here, $\Delta z = L/1000$ was chosen.

The left column shows the corresponding concentration profiles. Wherever applicable, we have also marked the computed heights of the supernate-suspension interface, $z_0(t)$, and of the suspension-sediment interface, $z_c(t)$. The last time has been chosen so large that both coincide, i.e. the solid component is entirely contained in the sediment.

The right column shows plots of instantaneous solid and fluid particle paths, which are plotted by large and small dots, respectively. To construct these paths, we consider the velocity field $\mathbf{q}$ and the concentration distribution ϕ (and thus the velocity fields $\mathbf{v}_s$ and $\mathbf{v}_f$) to be stationary at the time t. We denote by τ a time parameter for the construction of the instantaneous particle paths. The solid particle paths start from $x_s(\tau = 0) = 0.1k - 0.05\,[\mathrm{m}]$, $k = 1, \ldots, 5$, $z_s(\tau = 0) = 1\,[\mathrm{m}]$, and are continued by the polygonal method

$$x_s(\tau + \Delta\tau) = x_s(\tau) + \Delta\tau v_{sx}(x_s, z_s), \quad z_s(\tau + \Delta\tau) = z_s(\tau) + \Delta\tau v_{sz}(x_s, z_s),$$

where $v_{sx}(x_s, z_s)$ and $v_{sz}(x_s, z_s)$ are calculated from the fields q_z and ϕ by (40a) and (40c) (where we set $\theta = 0$). Taking into account the kinematic relationship (2), local values of v_{f_x} and v_{f_z} can be computed in a similar fashion and be used for the construction of fluid particle paths. Here, we construct two families of fluid particle paths: particle paths starting from different points of the top of the vessel ($x_f(\tau = 0) = 0.4 \cdot 2^{k-6}\,[\mathrm{m}]$, $k = 1, \ldots, 6$; $z_f(\tau = 0) = 1\,[\mathrm{m}]$) and from near its bottom ($x_f(\tau = 0) = 0.8 \cdot 2^{k-6}\,[\mathrm{m}]$, $k = 1, \ldots, 6$; $z_f(\tau = 0) = 0.01\,[\mathrm{m}]$). In this and the following example (Fig. 7), the distance between two plotted dots of each

path corresponds to the distance traveled in $\Delta\tau = 100\,[\mathrm{s}]$ for $z > z_c(t)$ and in $50\Delta\tau = 5000\,[\mathrm{s}]$ for $z \le z_c(t)$, respectively.

We observe that the solid particle trajectories have the same shape for all times, i.e. are straight lines intersecting at the cone tip ($x = 0$, $z = 2\,[\mathrm{m}]$). However, velocities vary substantially along these lines. In particular, velocities diminish drastically when the solid particle paths enters the consolidation zone ($z < z_c(t)$).

The fluid particle trajectories show very interesting behaviour. Both families indicate that fluid flow directed towards the inclined boundary. The fluid particle trajectories drawn for $t = 0$ are very similar to those of SCHNEIDER's Figure 5 [46]. Moreover, fluid velocities in the clear liquid region ($z > z_0(t)$) tend to be very high. Apparently, over the entire height $0 \le z \le H$, fluid leaves the vessel through the inclined boundary. To quantify this effect, we define the boundary fluid flux density

$$\psi_{\mathrm{f}}(z,t) = -\frac{2\pi r(z)}{\|\mathbf{n}(z)\|\big(1+r'(z)\big)^{1/2}}\big(1-\phi(z,t)\big)\mathbf{v}_{\mathrm{f}}\big(r(z),z,t\big)\cdot\mathbf{n}(z). \tag{78}$$

Obviously, the total amount of fluid leaving through the boundary between two heights z_1 and z_2 at time t is given by

$$\int_{z_1}^{z_2} \psi_{\mathrm{f}}(z,t)\,dz.$$

In the middle column of Figure 5 we have plotted profiles of ψ_{f}. An obvious result is that most fluid leaves through the boundary in the clear liquid zone, and that this effect becomes absent at the boundary corresponding to the sediment zone as consolidation proceeds. The only thinkable physical explanation of this phenomenon is, of course, the existence of a boundary layer through which fluid streams upwards and re-enters the vessel through its top. Although this mechanism seems quite absurd, it provides a method to verify the conservativity of the numerical method: requiring that all liquid leaving through the lateral boundary of the conical vessel comes back through the flat top implies that the error

$$\epsilon_{\mathrm{f}} = \left| 1 - \frac{1}{2\pi r(H)^2 \big|\widetilde{v_{\mathrm{f}z}}(H,t)\big|} \int_0^H \widetilde{\psi}_{\mathrm{f}}(z,t)\,dz \right|$$

should remain small (since the distinction is essential here, the tilde denotes numerically computed values of a quantity). This is a consequence of the continuity equation of the fluid. For the examples presented in Figure 6, we found $\epsilon_{\mathrm{f}} = 0.072$ for $t = 0$, $\epsilon_{\mathrm{f}} = 0.00067$ for $t = 2000\,[\mathrm{s}]$ and $\epsilon_{\mathrm{f}} = 0.00045$ for $t = 12000\,[\mathrm{s}]$, respectively.

4.2 Sedimentation between inclined walls

In the second example, we consider an initially homogeneous suspension, again of initial concentration $\phi_0 = 0.05$, in a two-dimensional vessel of height $H = 1\,[\mathrm{m}]$ with inclined parallel walls and $\alpha = 63.435°$. In the left column of Figure 7, we show the

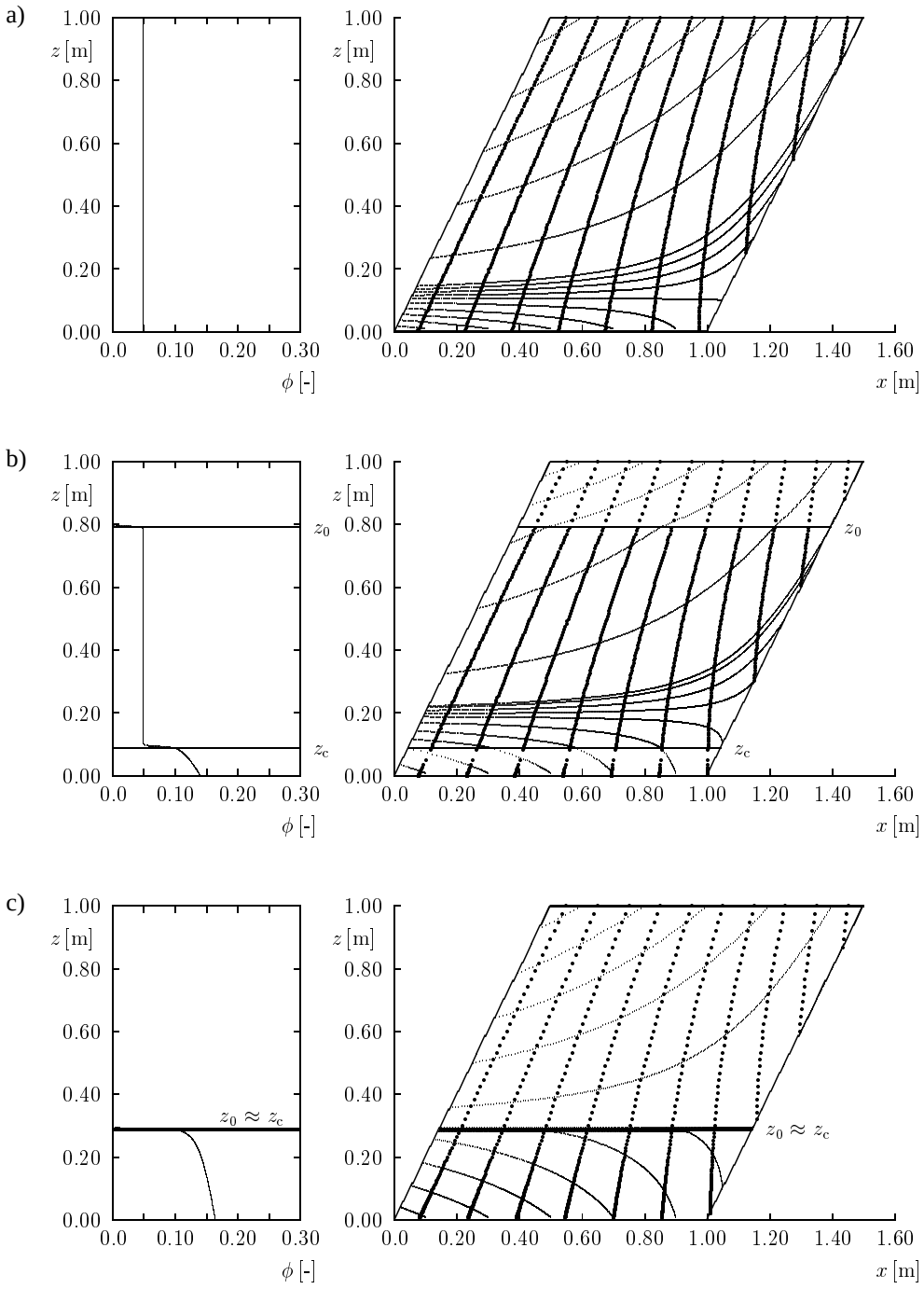

Figure 7: Simulation of sedimentation between parallel walls with inclination angle $\alpha = 63.425°$: concentration profiles (left) and solid (fat dots) and fluid particle paths (right) at times (a) $t = 0$, (b) $t = 2000$ [s] and (c) $t = 12000$ [s].

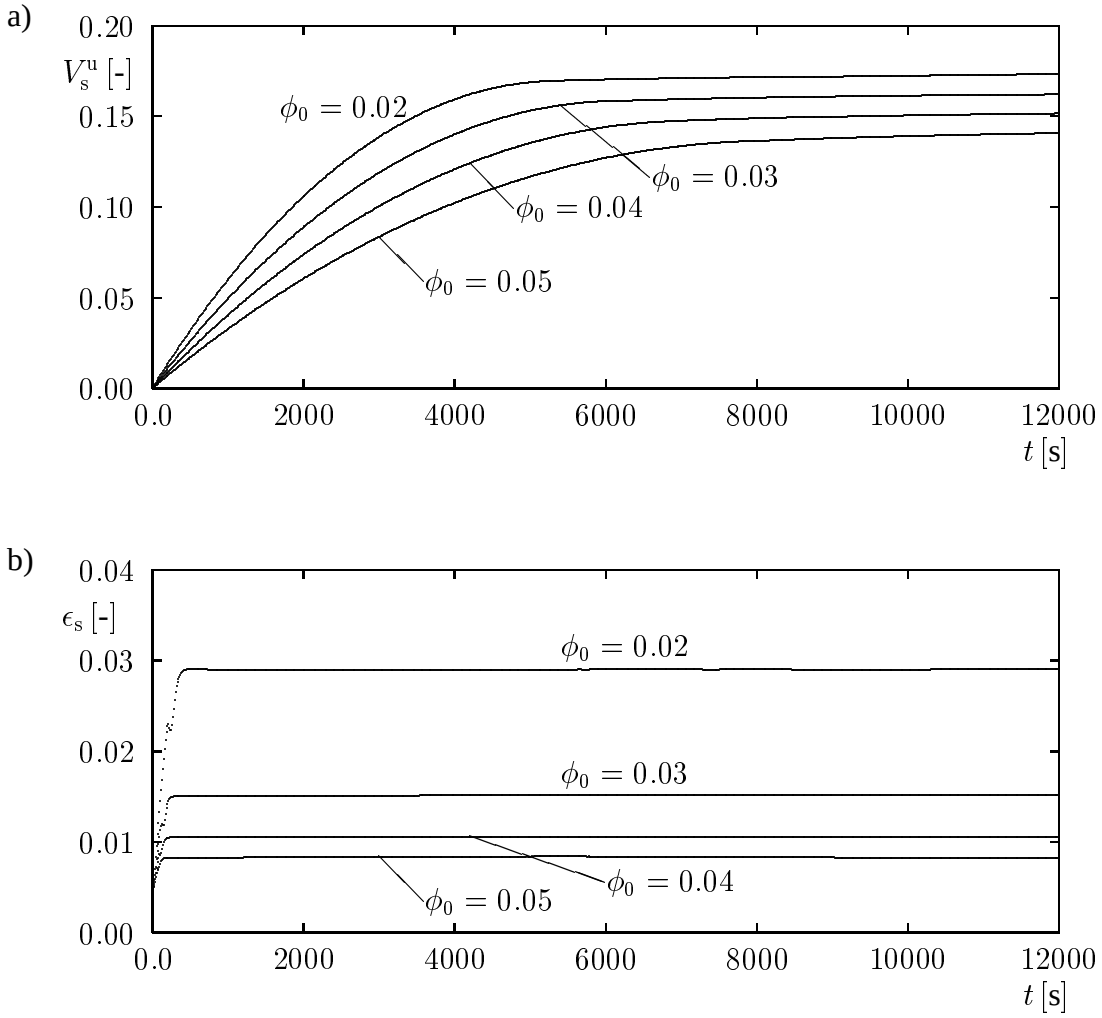

Figure 8: Simulation of sedimentation between parallel walls: (a) cumulated volume of solids V_s^u having left the vessel through the upward-facing wall, (b) relative mass error ϵ_s as a function of time for four different initial concentrations.

concentration profiles of at (a) $t = 0$, (b) $t = 2000\,[\mathrm{s}]$ and (c) $t = 12000\,[\mathrm{s}]$. The right column shows the plots of the instantaneous solid and fluid particle paths which have been obtained in the same way as for the previous example. The plotted solid particle paths start from $x_\mathrm{s}(\tau = 0) = 1.05 + 0.1(k-1)\,[\mathrm{m}]$, $k = 1, \ldots, 10$, $z_\mathrm{s}(\tau = 0) = 1\,[\mathrm{m}]$, while the fluid particle paths start from different points of the top of the vessel ($x_\mathrm{f}(\tau = 0) = 0.6 + 0.2(k-1)\,[\mathrm{m}]$, $k = 1, \ldots, 5$; $z_\mathrm{f}(\tau = 0) = 1\,[\mathrm{m}]$), from the upward-facing inclined wall ($x_\mathrm{f}(\tau = 0) = 1.05 + 0.1(k-1)\,[\mathrm{m}]$, $z_\mathrm{f}(\tau = 0) = 0.1 + 0.2(k-1)\,[\mathrm{m}]$, $k = 1, \ldots, 5$) and from near its bottom ($x_\mathrm{f}(\tau = 0) = 0.1 + 0.2(k-1)\,[\mathrm{m}]$, $k = 1, \ldots, 5$; $z_\mathrm{f}(\tau = 0) = 0.01\,[\mathrm{m}]$). The trajectories for $t = 0$ can be compared with those plotted in Figure 8 of SCHNEIDER [46]. However, since the initial concentration is not zero, we obtain additional details of the instantaneous flow field. In particular, since we the upward-facing wall is assumed to be impermeable to the mixture, any flow of solids "through" that boundary (this effect is explained by the formation of a boundary layer) has to be balanced by an inflow of the same volume of liquid. For the transient flow fields plotted in Figure 7a) and b), we therefore obtain a family of fluid particle trajectories directed away from the upward-facing inclined wall. The plot for $t = 12000\,[\mathrm{s}]$ illustrates that there are no such trajectories in the clear liquid zone, from which of course no solids can settle out through the boundary. Moreover, by the density of plotted dots, we observe that velocities in the compression zone are very small.

For this configuration, we measured the volume of solids (relative to the initial volume of solids) that have left the vessel through the upward-facing wall at time t by

$$V_\mathrm{s}^\mathrm{u}(t) = -\frac{1}{\phi_0 L}\int_0^t \int_0^H \frac{\phi(z,\tau)}{\|\mathbf{n}_+(z)\|\big(1 + x'_+(z)\big)^{1/2}}\mathbf{v}_\mathrm{s}\big(x_+(z), z, \tau\big)\mathbf{n}_+(z)\,dz d\tau. \qquad (79)$$

This quantity has been determined for four runs with different initial concentrations and is plotted in Figure 8a). We can observe that for initial concentrations varying between 0.02 and 0.05, between 14% and 17.4% of the initial solids volume is caught in the boundary layer after $t = 12000\,[\mathrm{s}]$. For $\phi_0 = 0.02$, the settling process is terminated most rapidly, and the corresponding curve is the first to take almost horizontal shape.

Of course, the continuity equation for the solid implies that at any time $t > 0$, $V_\mathrm{s}^\mathrm{u}(t)$ plus the volume of solids contained *in* the tank at that time gives the initial solids volume. However, due to numerical errors this not exactly true. To check the conservativity of the numerical method, we also determined the relative mass error

$$\epsilon_\mathrm{s}(t) = 1 - \widetilde{V_\mathrm{s}^\mathrm{u}}(t) - \frac{1}{\phi_0 L}\int_0^H \widetilde{\phi}(z,t)dz, \qquad (80)$$

which is plotted in Figure 8b) for the four initial concentrations of Figure 8a). (The use of the tilde is the same as in equation (79).) This quantity depends, of course, on the discretization parameters, and numerical experiments have shown that $\|\epsilon_\mathrm{s}\|_\infty \to 0$ for $\Delta z \to 0$ when the mesh size ratio $\Delta z/\Delta t$ remains constant. However,

for the fixed value $\Delta z = H/1000$ considered here, it is interesting to note that this error builds up rapidly during a very small initial time interval, and then remains almost constant. This behaviour is possibly due to the splitting error present in the solution algorithm when ϕ varies rapidly, as is the case for small times.

For $\phi_0 = 0.05$, the error ϵ_s remains roughly constant at 0.8% for $\Delta z = H/1000$, and numerical experiments have shown that $\|\epsilon_s\|_\infty \to 0$ for $\Delta z \to 0$. This error is considerably higher for lower initial concentrations, but shows the same qualitative behaviour.

5 Conclusions

We concluded from the general field equations that it is impossible to prescribe both boundary conditions for the solid and the liquid phase at the boundary of a closed vessel simultaneously. We have demonstrated that this deficiency can not be explained by the presence of boundary layers of clear liquid beneath downward-facing and of sediment on upward-facing inclined walls:

A detailed analytical study of the velocity fields of both phases leads to the conclusion that these flow fields are immediately influenced by distant inclined boundaries for a very small initial time $t \to 0$, even in those regions in the interior of the vessel, where we expect simple vertical flow fields. Consider for example a conical vessel and an initially homogeneous solid concentration. In this case, in experiments such as those of SCHAFLINGER [45] flow of clear liquid in a thin (compared to the diameter of the vessel) boundary layer beneath the downward-facing walls is observed. However, the presence of such boundary layers can not explain that the flow fields are not correct far away from the boundaries.

Similar problems occur for the final consolidation state when $t \to \infty$, where we obtain a flow field of clear liquid which circulates for infinite time through the inclined walls and the top of the vessel, despite the fact that we have assumed a vessel which is impermeable for both phases. In this case the fluid should be at rest and there is no boundary layer which could explain this absurd result. Exactly the same problems for $t \to 0$ and $t \to \infty$ arise in the study of Schneider [46].

The reason for this difficulty is in fact a deficiency of the general field equations, in particular of the simple form of the linear momentum balance (7), which led to the conclusion that the concentration of the solid does only depend on z and t and that the boundary conditions for both phases can not be satisfied simultaneously for a closed vessel. Consequently, an improved set of model equations should include a more elaborate linear momentum balance (such as that presented in [13]) in which additional advective acceleration or viscosity terms are retained. Such a formulation also implies that the interaction of the kinematic waves, i.e. of the evolution of the concentration distribution, with the volume average velocity field of the mixture, is modeled in the whole vessel, whereas this interaction is modeled here merely via boundary conditions. The boundary conditions should supplement the general field

equations, and not be part of these. Of course, such a modification of the present model requires the solution of truly multidimensional equations, and rules out simple one-dimensional numerical solution procedures such as that employed here.

Despite the fact that the present model produces incorrect flow fields, it is mathematically sound and can be solved numerically quite easily. Moreover, the corresponding concentration profiles are in qualitative agreement with observations of enhanced settling rates in vessels with inclined walls. (In this context, it is interesting to note that the numerical experiments did not predict that inclined walls cause an increase in the final bottom concentration.) It should therefore be interesting to analyze whether the concentration profiles calculated here may at least be considered as useful approximations of concentration profiles of improved model equations. Unfortunately, most experimental evidence for such a hypothesis is related to incompressible (unflocculated) mono- or polydisperse suspensions [18, 32, 45]. Experiments with flocculated slurries beneath inclined walls seem to be lacking, although such materials are widely used in the mineral industries.

Acknowledgements

We acknowledge support by the Collaborative Research Programme (Sonderforschungsbereich) 404 at the University of Stuttgart. Raimund Bürger would like to thank the group of Prof. K. Wilmański at the Weierstraß Institute for great hospitality. Thanks are due to Mr Philipp Walter who helped us to obtain some of the references.

References

[1] Acrivos, A.; Herbolzheimer, E.: Enhanced sedimentation in settling tanks with inclined walls, J. Fluid Mech. **92** (1979), 435–457.

[2] Amberg, G.; Dahlkild, A.A.: Sediment transport during unsteady settling in an inclined channel, J. Fluid Mech. **185** (1987), 415–436.

[3] Bedford, A; Hill, C.D.: A mixture theory formulation for particulate sedimentation, AIChE J. **22** (1976), 938–940.

[4] Borhan, A.; Acrivos, A.: The sedimentation of nondilute suspensions in inclined settlers, Phys. Fluids **31** (1988), 3488–3501.

[5] Boycott, A.E.: Sedimentation of blood corpuscules, Nature **104** (1920), 532.

[6] Bürger, R.; Bustos, M.C.; Concha, F.: Settling velocities of particulate systems: 9. Phenomenological theory of sedimentation processes: numerical simulation of the transient behaviour of flocculated suspensions in an ideal batch or continuous thickener, Int. J. Mineral Process. **55** (1999), 267–282.

[7] Bürger, R; Concha, F.: Mathematical model and numerical simulation of the settling of flocculated suspensions. Int. J. Multiphase Flow **24** (1998), 1005–1023.

[8] Bürger, R.; Concha, F.; Tiller, F.M.: Application of the phenomenological theory to several published experimental cases of sedimentation processes, Separ. Purif. Technol., to appear in a special issue.

[9] Bürger, R.; Evje, S.; Karlsen, K.H.: On strongly degenerate convection-diffusion problems modeling sedimentation-consolidation processes, Applied Mathematics Report, University of Bergen, Bergen, Norway, 1999, submitted to SIAM J. Math. Anal.

[10] Bürger, R.; Evje, S.; Karlsen, K.H.; Lie, K.-A.: Numerical methods for the simulation of the settling of flocculated suspensions, Separ. Purif. Technol., to appear in a special issue.

[11] Bürger, R.; Karlsen, K.H.: Analysis and numerics of strongly degenerate convection-diffusion problems modeling sedimentation-consolidation processes, Proceedings of MAFELAP 1999, to appear.

[12] Bürger, R.; Karlsen, K.H.: On some finite difference schemes for the phenomenological sedimentation-consolidation model, Applied Mathematics Report, University of Bergen, Bergen, Norway, in preparation.

[13] Bürger, R.; Wendland, W.L.; Concha, F.: Model equations for gravitational sedimentation-consolidation processes, Z. Angew. Math. Mech. **80** (2000), 79–92.

[14] Bustos, M.C.; Concha, F.; Bürger, R.; Tory, E.M.: Sedimentation and Thickening, Kluwer Academic Publishers, Dordrecht, The Netherlands, 1999.

[15] Damasceno, J.J.R.; Henrique, H.M.; Massarani, G.: Análise do comportamento dinâmico de um espessador Dorr-Oliver, Proceedings of the *III Meeting of the Southern Hemisphere on Mineral Technology*, São Lourenço, MG, Brazil, September 13–16, 1992, 675–689.

[16] Damasceno, J.J.R.; Souza, R.; Massarani, G.: Determinação de parâmetros constitutivos para o espessamento utilizando a técnica de atenuação de raios gama, *XIX Encontro sobre Escoamento em Meios Porosos (XIX ENEMP)*, Campinas, SP, Brazil, 1991.

[17] Davis, R.H.; Acrivos, A.: Sedimentation of noncolloidal particles at low Reynolds numbers, *Ann. Rev. Fluid Mech.* **17** (1985), 91–118.

[18] Davis, R.H.; Herbolzheimer, E.; Acrivos, A.: The sedimentation of polydisperse suspensions in vessels having inclined walls, Int. J. Multiphase Flow **8** (1982), 571–585.

[19] Espedal, M.S.; Karlsen, K.H.: Numerical solution of reservoir flow problems based on large time step operator splitting algorithms, in: Fasano, A.; van Duijn, H (eds.): Filtration in Porous Media and Industrial Applications, Lecture Notes in Mathematics, Springer Verlag, to appear.

[20] Garrido, P.; Bürger, R.; Concha, F.: Settling velocities of particulate systems: 11. Comparison of the phenomenological sedimentation-consolidation model with published experimental results. Preprint 99/17, Sonderforschungsbereich 404, University of Stuttgart 1999, submitted to Int. J. Mineral Process.

[21] Graham, W.; Lama, R.: Sedimentation in inclined vessels, Can. J. Chem. Engrg. **41** (1963), 31–32.

[22] Graham, W.; Lama, R.: Continuous thickening in an inclined thickener, Can. J. Chem. Engrg. **41** (1963), 162–165.

[23] Herbolzheimer, E.; Acrivos, A.: Enhanced sedimentation in narrow tilted channels, J. Fluid Mech. **108** (1981), 485–499.

[24] Hill, W.D.; Rothfus, R.R.; Li, K.: Boundary-enhanced sedimentation due to settling convection, Int. J. Multiphase Flow **3** (1977), 561–583.

[25] Holden, H.; Karlsen, K.H.; Lie, K.-A.: Operator splitting methods for degenerate convection-diffusion equations I: convergence and entropy estimates, Preprint, University of Bergen, Bergen, Norway.

[26] Holden, H.; Karlsen, K.H.; Lie, K.-A.: Operator splitting methods for degenerate convection-diffusion equations II: numerical examples with emphasis on reservoir simulation and sedimentation, Preprint, University of Bergen, Bergen, Norway.

[27] Inouye, K.; Uchibori, T.; Katsurai, T.: Über die Beschleunigung der Sedimentation im Gefäß, welches aus zwei Röhren von verschiedenen Durchmessern besteht. Kolloid-Z. **139** (1954), 167–170.

[28] Kapoor, B.; Acrivos, A.: Sedimentation and sediment flow in settling tanks with inclined walls, J. Fluid Mech. **290** (1995), 39–66.

[29] Kinosita, K.: Sedimentation in tilted vessels (1), J. Colloids **4** (1949), 525–536.

[30] Kynch, G.J.: A theory of sedimentation, Trans. Faraday Soc. **48** (1952), 166–176.

[31] Landman, K.A.; White, L.R.: Solid/liquid separation of flocculated suspensions, Adv. Colloid Interf. Sci. **51** (1994), 175–246.

[32] Law, D.H.; MacTaggart, R.S.; Nandakumar, K.; Masliyah, J.H.: Settling behaviour of heavy and buoyant particles from a suspension in an inclined channel, J. Fluid Mech. **187** (1988), 301–318.

[33] Leung, W.; Probstein, R.F.: Lamella and tube settlers. 1. Model and operation, Ind. Eng. Chem. Process Des. Develop. **22** (1983), 58–67.

[34] Mace, G.R.; Laks, R.: Developments in gravity separation, Chem. Engrg. Progr. **74** (7) (1978), 77–83.

[35] McCaffery, S.J.; Elliott, L.; Ingham, D.B.: Two-dimensional enhanced sedimentation in inclined fracture channels, Math. Engrg. Ind. **7** (1998), 97–125.

[36] Michaels, A.S.; Bolger, J.C.: Settling rates and sediment volumes of flocculated Kaolin suspensions, Ind. Engrg. Chem. Fund. **1** (1962), 24–33.

[37] Nakamura, H.; Kuroda, K.: La cause de l'accélération de la vitesse de sédimentation des suspensions dans les récipients inclinés, Keijo J. Med. **8** (1937), 256–296.

[38] Nir, A.; Acrivos, A.: Sedimentation and sediment flow on inclined surfaces, J. Fluid Mech. **212** (1990), 139–153.

[39] Oliver, D.R.: Continuous vertical and inclined settling of model suspensions, *Can. J. Chem. Engrg.* **42** (1964), 268–272.

[40] Oliver, D.R.; Jenson, V.G.: The inclined settling of dispersed suspensions of spherical particles in square-section tubes, Can. J. Chem. Engrg. **42** (1964), 191–195.

[41] Ponder, E.: On sedimentation and rouleaux formation, Quart. J. Exp. Physiol. **15** (1925), 235–252.

[42] Prasad, P.: Waves at the interface between a clear liquid and a mixture in a two-phase flow, J. Fluid Mech. **150**, 417–426.

[43] Richardson, J.F.; Zaki, W.N.: Sedimentation and fluidization I, Trans. Instn. Chem. Engrs. (London) **32** (1954), 35–53.

[44] Rushton, A.; Ward; A.S.; Holdich, R.G.: Solid-Liquid Filtration and Separation Technology. Second edition, Wiley-VCH, Weinheim, 2000.

[45] Schaflinger, U.: Experiments on sedimentation beneath downward-facing inclined walls, Int. J. Multiphase Flow **11**, 189–199.

[46] Schneider, W.: Kinematic-wave theory of sedimentation beneath inclined walls, J. Fluid Mech. **120** (1982), 323–346.

[47] Shaqfeh, E.S.G.; Acrivos, A.: The effects of inertia on the buoyancy-driven convection flow in settling vessels having inclined walls, Phys. Fluids **29** (1986), 3935–3948.

[48] Shaqfeh, E.S.G.; Acrivos, A.: The effects of inertia on the stability of the convective flow in inclined particle settlers, Phys. Fluids **30** (1987), 960–973.

[49] Shaqfeh, E.S.G.; Acrivos, A.: Enhanced sedimentation in vessels with inclined walls: experimental observations, Phys. Fluids **30** (1987), 1905–1914.

[50] Zahavi, E.; Rubin, E.: Settling of solid suspensions under and between inclined surfaces, Ind. Engrg. Chem. Process Des. Develop. **14** (1975), 34–41.